Incident fractures of the distal radius: Dual-energy CT-derived metrics for opportunistic risk stratification

Leon D. Gruenewald [a], Christian Booz [a], Jennifer Gotta [a], Philipp Reschke [a], Simon S. Martin [a], Scherwin Mahmoudi [a], Simon Bernatz [a], Katrin Eichler [a], Tommaso D'Angelo [b], Victoria Chernyak [c], Christof M. Sommer [d,*], Thomas J. Vogl [a], Vitali Koch [a]

[a] Goethe University Frankfurt, University Hospital, Department of Diagnostic and Interventional Radiology, Frankfurt am Main, Germany
[b] Department of Biomedical Sciences and Morphological and Functional Imaging, University Hospital Messina, Messina, Italy
[c] Department of Radiology, Memorial Sloan Kettering Cancer Center, New York City, NY, USA
[d] Clinic of Diagnostic and Interventional Radiology, Heidelberg University Hospital, Heidelberg, Germany

ARTICLE INFO

ABSTRACT

Background: Dual-energy CT (DECT)-derived bone mineral density (BMD) of the distal radius and other CT-derived metrics related to bone health have been suggested for opportunistic osteoporosis screening and risk evaluation for sustaining distal radius fractures (DRFs).
Methods: The distal radius of patients who underwent DECT between 01/2016 and 08/2021 was retrospectively analyzed. Cortical Hounsfield Unit (HU), trabecular HU, cortical thickness, and DECT-based BMD were acquired from a non-fractured, metaphyseal area in all examinations. Receiver-operating characteristic (ROC) analysis was conducted to determine the area under the curve (AUC) values for predicting DRFs based on DECT-derived BMD, HU values, and cortical thickness. Logistic regression models were then employed to assess the associations of these parameters with the occurrence of DRFs.
Results: In this study, 263 patients (median age: 52 years; interquartile range: 36–64; 132 women; 192 fractures) were included. ROC curve analysis revealed a higher area under the curve (AUC) value for DECT-derived BMD compared to cortical HU, trabecular HU, and cortical thickness (0.91 vs. 0.61, 0.64, and 0.69, respectively; $p < .001$). Logistic regression models confirmed the association between lower DECT-derived BMD and the occurrence of DRFs (Odds Ratio, 0.83; $p < .001$); however, no influence was observed for cortical HU, trabecular HU, or cortical thickness.
Conclusions: DECT can be used to assess the BMD of the distal radius without dedicated equipment such as calibration phantoms to increase the detection rates of osteoporosis and stratify the individual risk to sustain DRFs. In contrast, assessing HU-based values and cortical thickness does not provide clinical benefit.

1. Introduction

Distal radius fractures (DRFs) are among the most encountered fractures in emergency departments. Over the past years, the incidence of DRFs has been rising steadily and is likely to continue to rise in the aging western population [1,2]. While the association of reduced bone mineral density (BMD) and incident fractures of the distal radius and other regions of the body is well established, the estimated number of patients with unrecognized osteoporosis remains unacceptably high, even after patients have sustained an osteoporosis-associated fracture [3].

Dual x-ray absorptiometry (DXA) is still considered the diagnostic gold standard for the diagnosis of osteoporosis despite well-established imitations such as inaccurate BMD measurements due to variations in body composition and vascular calcifications [4–6]. Consequently, the individual fracture risk derived from DXA-based BMD measurements has

---

been shown to be vastly inaccurate, with many fragility fractures occurring in patients with high areal BMD (aBMD) [7]. To overcome the aforementioned limitations, CT-based solutions that allow direct visualization of the bone structure and assessment of the true volumetric BMD, such as quantitative computed tomography (QCT) and peripheral quantitative computed tomography (pQCT), have been developed [8,9]. Both methods have been shown to provide accurate results for volumetric BMD assessment and incident fracture prediction, with lower radiation doses reported for pQCT [9,10]. However, both examinations also require dedicated equipment, such as calibration phantoms or specialized scanners, which hinders their application in clinical routine [11]. To allow for large-scale osteoporosis screening, simpler methods that facilitate retrospective BMD assessment are required. Different approaches have been suggested in this context, such as simple Hounsfield units (HU) measurements, asynchronous use of calibration phantoms, and aBMD measurements derived from scout views [8,12–14]. While these approaches correlate well with phantom-based HU measurements or DXA examinations, it is important to note that distortion by intravenous or oral contrast agents and overlying fat remains problematic, and calibrated volumetric BMD values are not obtainable [14]. In this context, a dual-energy CT (DECT)-based postprocessing algorithm based on three-material differentiation has recently been validated for predicting osteoporosis-associated fractures, including DRFs and potential complications such as bone non-union [15–20]. Together with other applications of material differentiation, for example the visualization of bone marrow edema and collagen-rich structures such as the triangular fibrocartilage complex, DECT could therefore serve as a

multi-purpose tool for the diagnosis of acute injury, degenerative changes and osteoporosis assessment in radiological practice in the future [21–24,34]. Due to the limited distribution of DECT scanners, this technique is currently only accessible by specialized clinics and, therefore, not suited for widespread application.

This study aimed to compare CT-derived bone-quality metrics that can be derived from both DECT and conventional CT for their value in assessing the risk of sustaining DRFs.

2. Materials and methods

The institutional review board approved the retrospective, monocentric study. The requirement to obtain written informed consent was waived.

2.1. Patient selection and study design

All patients who underwent unenhanced dual-source DECT of the distal radius between January 2016 and December 2022 were considered for study inclusion. Exclusion criteria were severe destruction of the distal radius (>75 %) as described below, suspected malignancy, and metallic implants. The Standard for Reporting Diagnostic Accuracy (STARD) flow chart of patient inclusion is illustrated in Fig. 1.

2.2. Image protocol

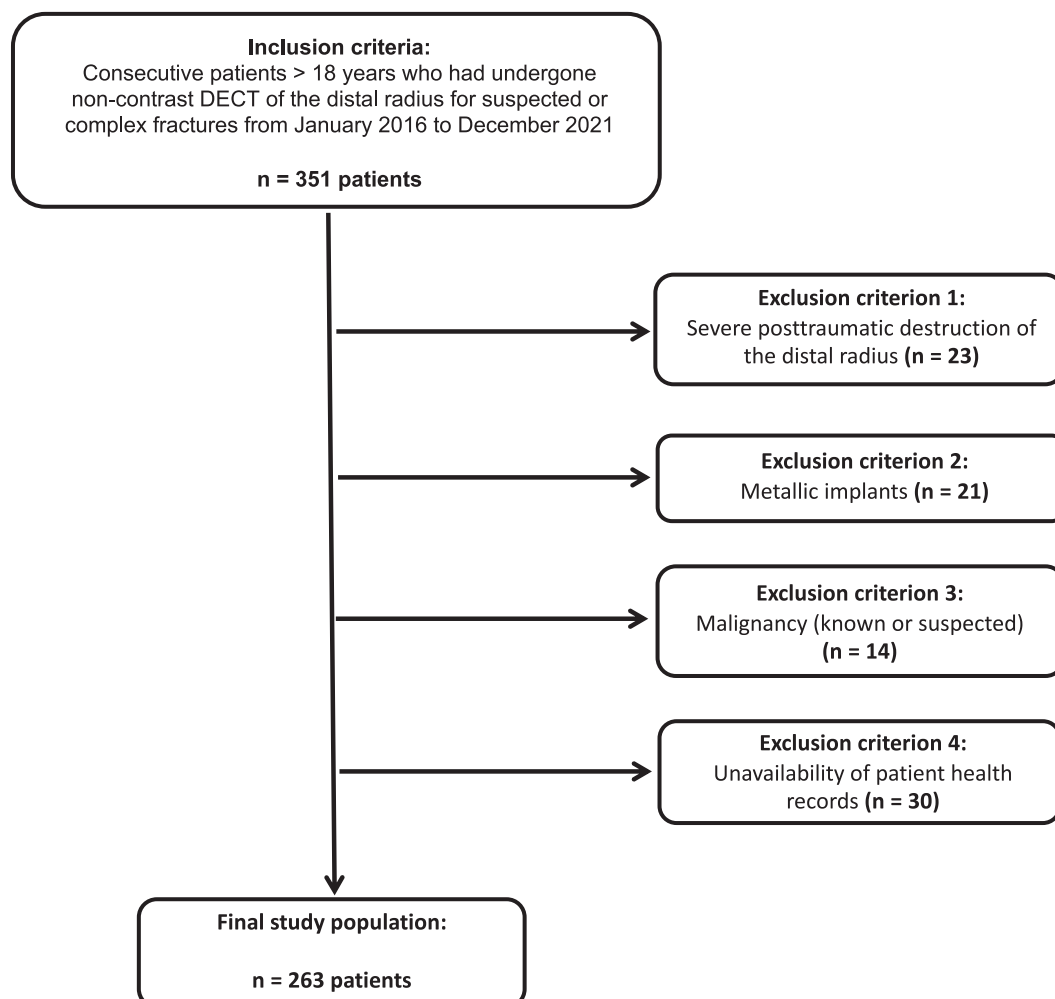All examinations were performed on a third-generation dual-source

Fig. 1. Standards for Reporting of Diagnostic Accuracy Studies Flow Chart of Patient Inclusion. Abbreviation: DECT = Dual-energy CT.

DECT device in dual-energy mode (SOMATOM Force; Siemens Healthineers, Forchheim, Germany). Two x-ray tubes operated at different kV settings (tube 1: 90 kVp, 180 mAs; tube 2: 150 kVp with 0.64 mm tin filter, 180 mAs). Image series were collected in a cranio-caudal direction. All examinations were performed without the administration of an intravenous contrast agent.

2.3. Image reconstruction

Three image sets were acquired in each examination: 90 kVp, 150 kVp, and weighted average (ratio, 0.5:0.5). Axial, coronal, and sagittal image series (thickness 1 mm, increment 0.75 mm) were reconstructed with a dedicated dual-energy bone kernel (Br69f) for image analysis and evaluation. All image series were automatically transferred to the picture archiving and communication system (PACS; General Electrics).

2.4. Image interpretation

Two board-certified radiologists with 15 and 7 years of experience in musculoskeletal imaging (K.E. and S.S.M.) evaluated all acquired CT images independent of all clinical information contained in the electronic patient files for the presence of a DRF. In case of divergent ratings, a third radiologist with ten years of experience in musculoskeletal imaging (T.D.) was consulted. Reported is the majority decision.

2.5. Bone assessment

CT metrics for bone quality were evaluated manually by two readers (S.M. and P.R.) with six and four years of experience in musculoskeletal radiology.

To normalize the location, area, and volume for bone quality measurements, a line (a) was plotted from the styloid process of the radius to the distal radio-ulnar joint, and its length was obtained. A second line measuring half the length of line (a) was then plotted in proximal direction along the medial border of the radius (b). The end of line (b) was used to construct a rectangle with the height of line (b), spanning the distal radius and centered at the end of line (b) (Fig. 2).

For DECT-based BMD analysis, the largest possible non-fractured segment within this rectangle was manually delineated throughout the entire stack of 2D slices to obtain a three-dimensional ROI for each patient. If the largest non-fractured segment had a volume of less than 25 % of the constructed rectangle, the examination was considered insufficient for BMD analysis, and the patient was excluded, as mentioned above. The three-dimensional ROI and both DECT image series were then used as input using a second software tool (BMD Analysis; Fraunhofer IGD). This software uses a dedicated material decomposition algorithm to obtain the BMD as previously described [15,16,20,25,26].

For trabecular HU measurements, the largest possible non-fractured
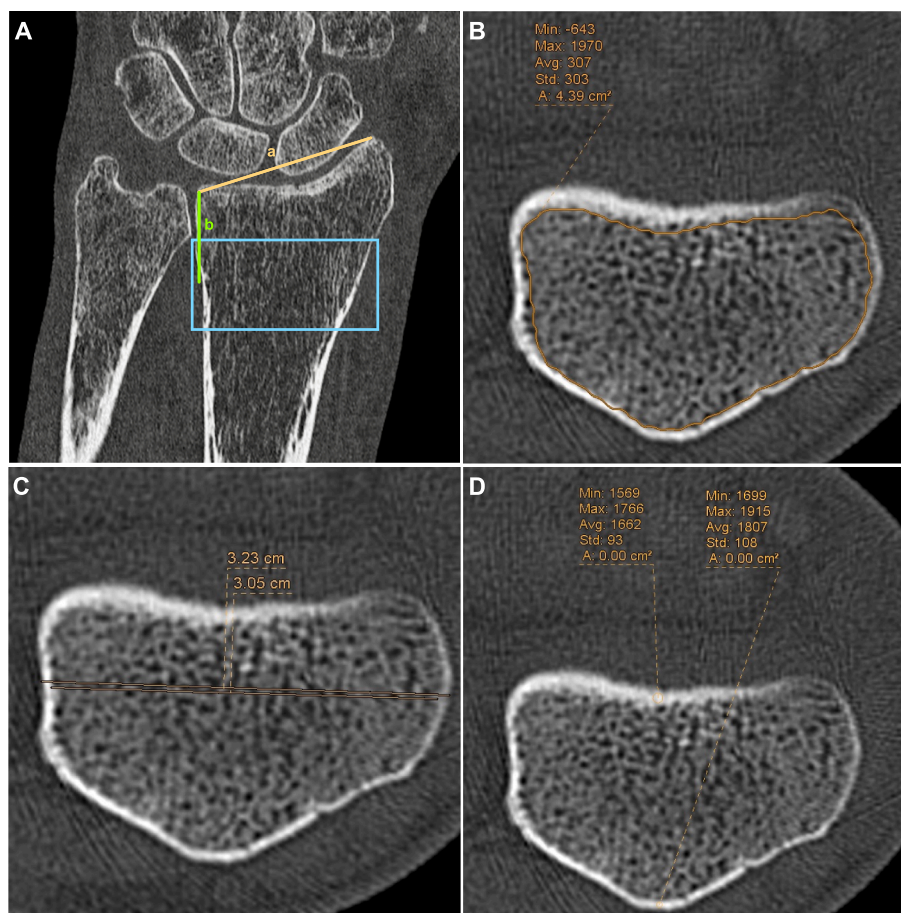
Fig. 2. Definition of the metaphyseal area of Interest. **(A)** To normalize the location for opportunistic BMD assessment, a line connecting the styloid process and the distal radio-ulnar joint was drawn (a). A second line (b) measuring half the length of line (a) was then drawn proximally along the medial border of the radius (b). The end of line (b) was used to construct a rectangle with the height of (b). **(B)** Within the rectangle, the trabecular bone was delineated throughout the entire stack of 2D slices to obtain a three-dimensional region of interest (ROI) for DECT-based BMD assessment. For trabecular HU assessment, the trabecular bone was delineated in the middle of the constructed rectangle. **(C)** Cortical thickness ratio was obtained by dividing the outside diameter of the radius by the inside diameter at the middle of the constructed rectangle. **(D)** Cortical HU values were obtained by manual measurement of the anterior and posterior corticalis at the middle of the constructed rectangle and calculating the mean value. Abbreviations: BMD = bone mineral density. DECT = dual-energy CT. HU = Hounsfield units.

area within the constructed rectangle was manually delineated, and the HU values were obtained. If the largest non-fractured segment spanned an area of less than 25 % of the constructed rectangle, the examination was considered insufficient for trabecular HU measurements, and the patient was excluded, as mentioned above.

For cortical HU measurements and cortical thickness ratio, non-fractured segments centred within the constructed rectangle were used. Cortical HU values were obtained by manual measurement anteriorly and posteriorly, and cortical thickness ratio was obtained by dividing the outside diameter of the radius by the inside diameter at the same height.

2.6. Statistical analysis

Statistical analysis was performed with dedicated software (Prism 9 for macOS, version 9.0.0, GraphPad Software LLC, San Diego; R, Windows Version 4.2.2, The R Foundation). Differences in baseline characteristics were assessed using t-tests, if applicable, or Mann-Whitney-tests, Chi-Squared-tests, and Kruskal-Wallis tests. Receiver-operating characteristic (ROC) curve analysis with calculation of the area under the curve (AUC) was performed to evaluate optimal BMD thresholds for the incidences of fractures, and logistic regression analysis was performed using a multivariable logistic regression model adjusted for covariables to analyze the relationship of volumetric BMD with the occurrence of DRFs. Reproducibility was evaluated using the intraclass correlation coefficient (ICC) in a 2-way mixed-effects model for absolute agreement. A p-value < 0.05 was regarded as statistically significant.

3. Results

351 patients underwent non-contrast third-generation dual-source DECT of the distal radius between January 2016 and December 2021. After the exclusion of 23 patients due to severe posttraumatic destruction of the distal radius, 21 patients due to metallic implants in the distal radius, 14 patients due to known or suspected malignancy, and 30 patients due to insufficient information in the electronic health records, the final study population consisted of 263 patients (median age, 52 years; interquartile range [IQR] 36 – 64; 132 women), of which 192 sustained a DRF.

3.1. Patient characteristics

Patients who sustained a DRF were significantly older (median age 55, IQR 43 – 67) compared to patients without fracture (median age 39, IQR 30 – 58, p <.001) and significantly more often female (p =.001). Scatter plots illustrating the patient distribution for all obtained metrics are given in Fig. 3.

The median DECT-derived BMD of the distal radius was 102.2 mg/cm^3 (IQR, 82.2 – 123.8 mg/cm^3). Patients without fracture had a significantly higher DECT-derived BMD than those with DRF (91.2 vs 134.2 mg/cm^3, p <.001). Trabecular HU (31 vs. 73, p <.001) and cortical HU (1688 vs 1780, p =.003) were also significantly higher in patients without DRF compared to those with DRFs. However, no significant differences were observed in cortical thickness ratio (1.36 vs 1.28, p =.11) (Fig. 4). Patient characteristics are given in Table 1.
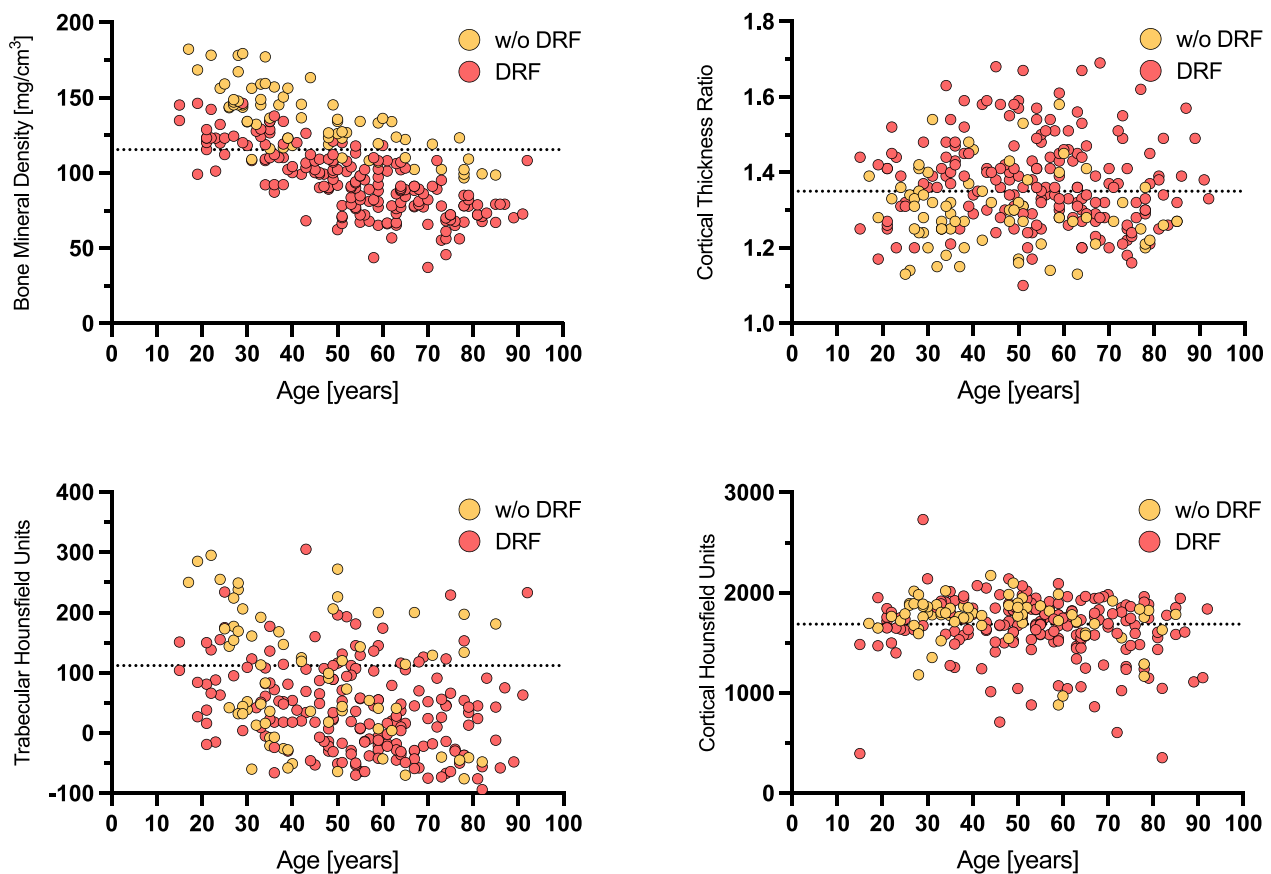
Fig. 3. Age and bone quality metrics of the study population. **(A-D)** Scatter plots illustrating the distribution of the obtained bone quality metrics and age. Red dots illustrate patients who sustained a distal radial fracture, and yellow dots illustrate patients without fracture. The dotted lines are optimized patient-level cutoffs for discrimination patients with DRF from patients without, as determined by ROC curve analysis. Abbreviations: DRF = distal radial fracture. ROC = receiver operator characteristic.
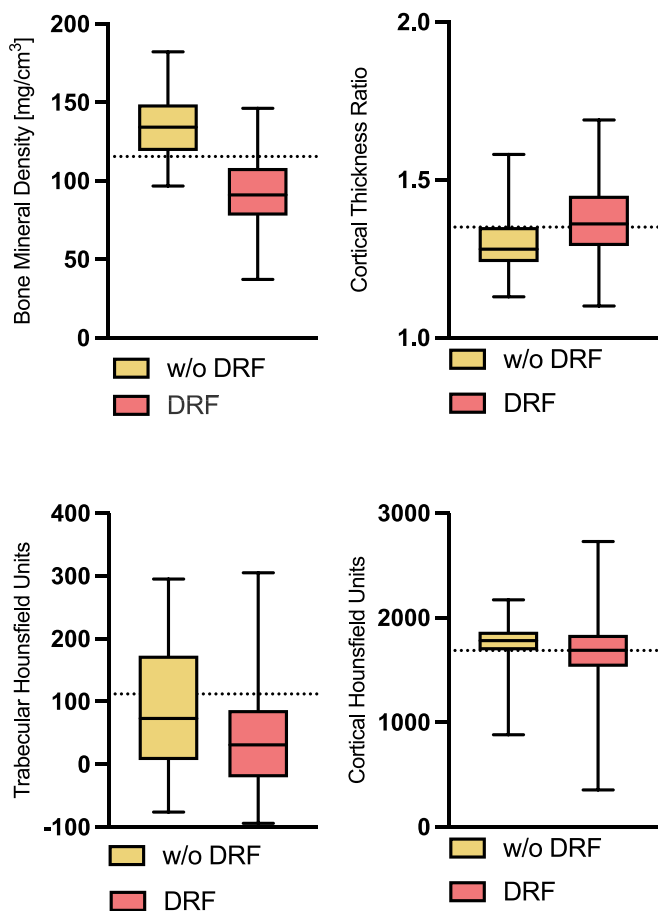
Fig. 4. Bone quality metrics in the study population. Box and whisker plots showing the bone quality metrics in patients who sustained a DRF and patients without. The dotted lines are optimized patient-level cutoffs for the identification of patients with DRF, as determined by ROC curve analysis. Abbreviations: DRF = distal radial fracture. ROC = receiver operator characteristic.

Table 1
Characterization of the patient population.

Variables - n (%)or median (IQR)	Total (n = 263)	DRF (n = 192)	No DRF (n = 71)	p-Value
Age (years)	52 (36 – 64)	55 (42.5 – 67)	39 (30 – 58)	<0.001
Sex (n)				0.001
• Male	131 (49.8 %)	84 (43.8 %)	47 (66.2 %)	
• Female	132 (50.2 %)	108 (56.2 %)	24 (33.8 %)	
DECT-derived BMD (mg/cm³)	102.2 (82.2 – 123.8)	91.2 (78.0 – 108.2)	134.2 (119.2 – 148.5)	<0.001
Trabecular HU	41.0 (-17.8 – 107.0)	31 (-20.0 – 85.5)	73 (8.5 – 172.0)	<0.001
Cortical HU	1735 (1578 – 1850)	1688 (1531 – 1837)	1780 (1690 – 1865)	0.003
Cortical Thickness Ratio	1.34 (1.27 – 1.42)	1.36 (1.29 – 1.45)	1.28 (1.24 – 1.35)	0.11

*Abbreviations: BMD. Bone Mineral Density; DRF. Distal Radius Fracture; HU. Hounsfield Units; IQR. Interquartile Range; Sex is given as number (percentage), all other values age given as median (IQR) after rejection of normality. Patients with a distal radial fracture were significantly older. significantly more often female and had significantly lower BMD. trabecular HU and cortical HU values. No significant difference was observed for the cortical thickness ratio.
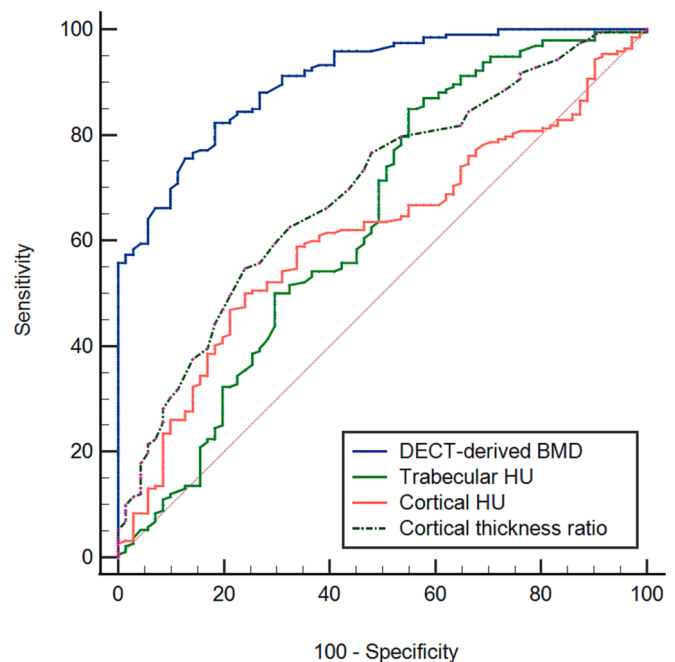
3.2. ROC curve analysis

ROC curve analysis of DECT-derived BMD values demonstrated high diagnostic accuracy with an AUC value of 0.91 (CI, 0.87 – 0.94, p <.001). A patient-level cut-off value ≤ 115.5 mg/cm³ yielded a sensitivity of 82.3 % (CI, 76.1 % – 87.4 %) and a specificity of 81.7 % (CI, 70.7 % – 89.9 %, p <.001) for identifying patients with DRF. Cortical thickness ratio, trabecular HU, and cortical HU values showed lower diagnostic accuracies with AUC values of 0.69 (p <.001), 0.64 (p =.001), and 0.61 (p =.003), respectively (Fig. 5). Detailed information, including optimal thresholds, sensitivity, and specificity, is provided in Table 2.

3.3. Logistic regression analysis

Logistic regression analyses were performed to examine the relationship between DECT-derived BMD, trabecular HU values, cortical HU values, and cortical thickness ratio with the occurrence of DRFs. An increase in DECT-derived BMD showed a protective effect against DRFs with an odds ratio of 0.83 (CI, 0.79–0.87; p <.001). Conversely, an increase in cortical thickness ratio was associated with an increased occurrence of DRFs (odds ratio 2140; CI, 105 – 58956; p <.001). Overall model quality was best for DECT-derived BMD with a Nagelkerkes R^2 of 0.74 compared to cortical thickness ratio (0.24), trabecular HU (0.14), and cortical HU (0.12). Integration of all parameters increased Nagelkerkes R^2 to 0.79. Detailed information is provided in Table 3. The overall model fit of all regression models was significant (p <.001).

3.4. Reproducibility of volumetric bone mineral density measurements

The interobserver agreement of all obtained metrics was generally high, but highest for trabecular HU and dual-energy CT derived BMD (ICC, 0.99 and 0.98, respectively), followed by cortical HU (ICC, 0.92) and cortical thickness ratio (ICC, 0.89) (Supplementary Table 1).

Fig. 5. ROC curve analysis of bone quality metrics. ROC curve analysis showed superior diagnostic accuracy for DECT-derived BMD (AUC = 0.91), versus trabecular HU (0.64), cortical HU (0.61), and cortical thickness ratio (0.69). Abbreviations: BMD = bone mineral density. DECT = dual-energy CT. HU = Hounsfield Units. ROC = receiver operator characteristic.

Table 2

ROC curve analysis of various CT-derived metrics for risk stratification to sustain distal radial fractures.

Metric	AUC	Youden Index	Sensitivity	Specificity	p-value
DECT-derived BMD	0.91 (0.87 – 0.94)	≤115.5	82.3	81.7	<0.001
Cortical Thickness Ratio	0.69 (64 – 0.75)	>1.35	54.7	76.1	<0.001
Trabecular HU	0.64 (0.58 – 0.69)	≤112	84.9	45.1	0.001
Cortical HU	0.61 (0.55 – 0.67)	≤1686	50.0	76.1	0.003

*Abbreviations: AUC. Area under the curve; BMD. Bone Mineral Density; HU. Hounsfield Units.

ROC-curve analysis demonstrates that DECT-derived BMD is superior to HU-based measurements and cortical thickness ratio for risk stratification of distal radial fractures. Numbers in brackets are confidence intervals.

Table 3

Logistic regression analysis of various CT-derived metrics for risk stratification to sustain distal radial fractures.

Metrics & Parameter	Coefficient	Odds Ratio	Nagelkerkes R^2	p-value
DECT-derived BMD			0.74	
• DECT-derived BMD	−0.18	0.83 (0.79–0.87)		<0.001
• Age	−0.13	0.87 (0.83–0.91)		<0.001
• Male Sex	−0.27	0.77 (0.27–2.07)		0.603
Cortical Thickness Ratio			0.24	0.063
• Cortical Thickness Ratio	7.67	2140 (105–58956)		<0.001
• Age	0.02	1.03 (1.01–1.04)		0.007
• Male Sex	0.77	2.16 (1.12–4.20)		0.022
Trabecular HU			0.14	
• Trabecular HU	−0.01	0.99 (0.99–1.00)		0.005
• Age	0.02	1.02 (1.00–1.04)		0.044
• Male Sex	0.42	1.52 (0.81–2.90)		0.195
Cortical HU			0.12	
• Cortical HU	0.00	1.00 (1.00–1.00)		0.063
• Age	0.02	1.02 (1.00–1.04)		0.018
• Male Sex	0.66	1.93 (1.04–3.61)		0.037
All Parameters			0.79	

*Abbreviations: BMD. Bone Mineral Density; HU. Hounsfield Units.

Logistic regression models show a protective effect of increased DECT-derived BMD, Trabecular HU, Cortical HU and Cortical thickness ratio against the occurrence of distal radial fractures. Numbers in brackets are confidence intervals. All regression models were statistically significant (p <.001), but goodness of fit was only high for DECT-derived BMD and a combined model using all parameters.

4. Discussion

Osteoporosis-associated fractures significantly contribute to morbidity and mortality in aging populations, with DRFs constituting the majority of such fractures [2]. The early identification of patients with inadequate bone health may facilitate the implementation of therapeutic interventions and lifestyle modifications to increase bone strength [27]. Here, we compared the utility of various CT-derived metrics of bone quality obtained from routine examinations of the distal radius for stratifying the risk of sustaining DRFs. Our results show that DECT-derived BMD assessment yields a significantly higher diagnostic accuracy for assessing fracture risk compared to those metrics that can be derived from conventional CT, such as cortical thickness ratio, trabecular HU values, and cortical HU values (0.91 vs 0.69, 0.64 and 0.61 respectively; p ≤ 0.003 for all metrics). Logistic regression analysis confirmed our findings with a high overall model fit for DECT-derived BMD but not all other values (p <.001 for all metrics).

Reported values for pQCT of the radius lie in the range of 155–180 mg/cm^3 in young patients and 100 – 140 mg/cm^3 in patients at the age of 80, which is slightly higher compared to the DECT-based approach used in this study [28], Possible explanations for the discrepancy include differences in image acquisition, such as a more distal measurement area for pQCT and the use of specialized equipment, the exclusion of patients with fractures, and technical effects attributable to dual-energy CT, such as the elimination of measurement inaccuracies like the fat error [29].

In contrast to DECT-derived BMD measurements, which showed the expected decline of BMD values among elderly patients, the distribution of all other metrics was overwhelmingly random [30]. While HU-based measurements have generally been shown to correlate with other methods to assess BMD in the spine, our results indicate that this correlation cannot be readily transferred to other body regions without prior validation [31]. Similarly, the cortical thickness ratio has previously been suggested as a valid surrogate metric for BMD based on measurements of the humerus, but we could not confirm this trend for the distal radius, where we observed no association between age and cortical thickness ratio [32]. While the divergent results in our study may be due to the uneven distribution of trabecular bone and cortical thickness in long tubular bones, which decrease from proximal to distal, this seems unlikely given a careful standardization of the measurement region and an overwhelmingly random distribution of the obtained values without correlation to DECT-based BMD.

In line with these findings, only DECT-derived BMD values provided good discrimination between patients who sustained a DRF and those who did not, indicating its suitability as a screening tool for osteoporosis, both in patients with DRF and patients without fractures. This finding carries significant clinical implications, as approximately 90 % of patients experiencing a distal radial fracture exhibit osteoporosis or osteopenia, and these fractures often serve as the initial symptom of the underlying bone-related condition [33]. Moreover, the application of this algorithm allows hospitals or radiological centers without dedicated pQCT equipment to perform BMD assessment at significantly lower radiation doses compared to conventional QCT, which represents a step forward in enhancing the diagnostic rate of low BMD. Cortical thickness ratio, trabecular HU values, and cortical HU values, in contrast, yielded only limited diagnostic value for identifying patients at risk of sustaining fractures. Nonetheless, trabecular HU yielded a sensitivity of 85 % to rule out osteoporosis without specialized equipment or dedicated software, even in fractured bones.

This study has limitations we want to address. Nearly all patients in our study cohort who underwent CT imaging of the radius had previously undergone X-ray imaging. This prior imaging either revealed a complex fracture or could not rule out an acute fracture. Consequently, our study population exhibited a preselection bias toward patients with and without complex fractures, and patients with uncomplicated fractures might be underrepresented. Furthermore, we observed a significant age gap between patients with and without distal radius fracture, which could be a confounding factor. Second, DECT-based BMD assessment uses a relatively large volumetric region of interest to extract the mineral content of the bone. In contrast, HU-based metrics and cortical thickness ratio were obtained at a single slice in the middle of the volumetric region of interest used for DECT-based BMD analysis. Given that the metaphyseal bone mineral density and the cortical thickness change from proximal to distal, this could have distorted the measurements. Third, we could not incorporate advanced analyses, such

as the evaluation of failure load, as a group of our study population already sustained fractures. Last, while the radiation dose of a CT of the wrist is relatively low, it is still significantly higher compared to a conventional x-ray of the wrist or DXA, and should only be performed after careful consideration.

In conclusion, we demonstrate a strong association of DECT-based BMD of the distal radius with the occurrence of distal radius fractures. DECT-based BMD can be obtained without dedicated equipment such as calibration phantoms, even when a fracture has been sustained. This approach can serve as a method to increase the detection rates of osteoporosis and stratify the individual risk to sustain DRFs. In contrast, assessing HU-based values and cortical thickness of the distal radius does not provide clinical benefit.

CRediT authorship contribution statement

Leon D. Gruenewald: Writing – original draft, Data curation, Formal analysis, Writing – review & editing. **Christian Booz:** Software. **Jennifer Gotta:** Formal analysis, Data curation. **Philipp Reschke:** Data curation, Writing – review & editing. **Simon S. Martin:** Writing – review & editing. **Scherwin Mahmoudi:** Writing – review & editing. **Simon Bernatz:** Writing – review & editing. **Katrin Eichler:** Supervision. **Tommaso D'Angelo:** Writing – review & editing. **Victoria Chernyak:** Conceptualization, Writing – review & editing. **Christof M. Sommer:** . **Thomas J. Vogl:** Supervision. **Vitali Koch:** Writing – original draft, Resources, Investigation, Conceptualization.

Declaration of competing interest

The authors declare that they have no known competing financial interests or personal relationships that could have appeared to influence the work reported in this paper.

Appendix A. Supplementary material

Supplementary data to this article can be found online at https://doi.org/10.1016/j.ejrad.2023.111283.

References

[1] K.W. Nellans, E. Kowalski, K.C. Chung, The epidemiology of distal radius fractures, Hand Clin. 28 (2) (2012) 113–125.
[2] J.A. Baron, M. Karagas, J. Barrett, W. Kniffin, D. Malenka, M. Mayor, et al., Basic epidemiology of fractures of the upper and lower limb among Americans over 65 years of age, Epidemiology. 7 (6) (1996) 612–618.
[3] E. Hernlund, A. Svedbom, M. Ivergard, J. Compston, C. Cooper, J. Stenmark, et al., Osteoporosis in the European Union: medical management, epidemiology and economic burden. A report prepared in collaboration with the International Osteoporosis Foundation (IOF) and the European Federation of Pharmaceutical Industry Associations (EFPIA), Arch Osteoporos. (2013).
[4] H.H. Bolotin, DXA in vivo BMD methodology: an erroneous and misleading research and clinical gauge of bone mineral status, bone fragility, and bone remodelling, Bone. 41 (1) (2007) 138–154.
[5] E.W. Yu, B.J. Thomas, J.K. Brown, J.S. Finkelstein, Simulated increases in body fat and errors in bone mineral density measurements by DXA and QCT, J Bone Miner Res. 27 (1) (2012) 119–124.
[6] N.R. Fuggle, E.M. Curtis, K.A. Ward, N.C. Harvey, E.M. Dennison, C. Cooper, Fracture prediction, imaging and screening in osteoporosis, Nature Publishing Group, Nature Reviews Endocrinology, 2019, pp. 535–547.
[7] S.C. Schuit, M. van der Klift, A.E. Weel, C.E. de Laet, H. Burger, E. Seeman, et al., Fracture incidence and association with bone mineral density in elderly men and women: the Rotterdam Study, Bone 34 (1) (2004) 195–202.
[8] M.T. Loffler, A. Jacob, A. Valentinitsch, A. Rienmuller, C. Zimmer, Y.M. Ryang, et al., Improved prediction of incident vertebral fractures using opportunistic QCT compared to DXA, Eur. Radiol. 29 (9) (2019) 4980–4989.
[9] W.H. Cheung, V.W. Hung, K.Y. Cheuk, W.W. Chau, K.K. Tsoi, R.M. Wong, et al., Best performance parameters of HR-pQCT to predict fragility fracture: systematic review and meta-analysis, J Bone Miner Res. 36 (12) (2021) 2381–2398.
[10] E. Sornay-Rendu, S. Boutroy, F. Duboeuf, R.D. Chapurlat, Bone microarchitecture assessed by HR-pQCT as predictor of fracture risk in postmenopausal women: the OFELY study, J Bone Miner Res. 32 (6) (2017) 1243–1251.
[11] S.J. Lee, P.M. Graffy, R.D. Zea, T.J. Ziemlewicz, P.J. Pickhardt, Future osteoporotic fracture risk related to lumbar vertebral trabecular attenuation measured at routine body CT, J Bone Miner Res. 33 (5) (2018) 860–867.
[12] P.J. Pickhardt, P.M. Graffy, R. Zea, S.J. Lee, J. Liu, V. Sandfort, et al., Automated abdominal CT imaging biomarkers for opportunistic prediction of future major osteoporotic fractures in asymptomatic adults, Radiology. 297 (1) (2020) 64–72.
[13] A. Laugerette, B.J. Schwaiger, K. Brown, L.C. Frerking, F.K. Kopp, K. Mei, et al., DXA-equivalent quantification of bone mineral density using dual-layer spectral CT scout scans, Eur Radiol. 29 (9) (2019) 4624–4634.
[14] K. Engelke, O. Chaudry, S. Bartenschlager, Opportunistic screening techniques for analysis of CT scans, Curr Osteoporos Rep. 21 (1) (2023) 65–76.
[15] L.D. Gruenewald, V. Koch, S.S. Martin, I. Yel, K. Eichler, T. Gruber-Rouh, et al., Diagnostic accuracy of quantitative dual-energy CT-based volumetric bone mineral density assessment for the prediction of osteoporosis-associated fractures, Eur Radiol. 32 (5) (2022) 3076–3084.
[16] L.D. Gruenewald, V. Koch, I. Yel, K. Eichler, T. Gruber-Rouh, L.S. Alizadeh, et al., Association of phantomless dual-energy CT-based volumetric bone mineral density with the prevalence of acute insufficiency fractures of the spine, Acad Radiol (2022).
[17] V. Koch, M.H. Albrecht, L.D. Gruenewald, I. Yel, K. Eichler, T. Gruber-Rouh, et al., Impact of intravenously injected contrast agent on bone mineral density measurement in dual-source dual-energy CT, Acad Radiol. 29 (6) (2022) 880–887.
[18] C. Booz, J. Noeske, M.H. Albrecht, L. Lenga, S.S. Martin, I. Yel, et al., Diagnostic accuracy of quantitative dual-energy CT-based bone mineral density assessment in comparison to Hounsfield unit measurements using dual x-ray absorptiometry as standard of reference, Eur J Radiol. 132 (2020) 109321.
[19] J.L. Wichmann, C. Booz, S. Wesarg, K. Kafchitsas, R.W. Bauer, J.M. Kerl, et al., Dual-energy CT-based phantomless in vivo three-dimensional bone mineral density assessment of the lumbar spine, Radiology. 271 (3) (2014) 778–784.
[20] L.D. Gruenewald, V. Koch, S.S. Martin, I. Yel, S. Mahmoudi, S. Bernatz, et al., Dual-energy CT-based opportunistic volumetric bone mineral density assessment of the distal radius, Radiology 308 (2) (2023) e223150.
[21] Z. Chen, Y. Chen, H. Zhang, X. Jia, X. Zheng, T. Zuo, Diagnostic accuracy of dual-energy computed tomography (DECT) to detect non-traumatic bone marrow edema: a systematic review and meta-analysis, Eur. J. Radiol. 153 (2022) 110359.
[22] L.D. Gruenewald, V. Koch, S.S. Martin, I. Yel, S. Mahmoudi, S. Bernatz, et al., Diagnostic value of DECT-based colored collagen maps for the assessment of cruciate ligaments in patients with acute trauma, Eur. Radiol. (2023).
[23] L.D. Gruenewald, D.H. Leitner, V. Koch, S.S. Martin, I. Yel, S. Mahmoudi, et al., Diagnostic value of DECT-based collagen mapping for assessing the distal tibiofibular syndesmosis in patients with acute trauma, Diagnostics (basel) 13 (3) (2023).
[24] V. Koch, F.C. Müller, K. Gosvig, M.H. Albrecht, I. Yel, L. Lenga, et al., Incremental diagnostic value of color-coded virtual non-calcium dual-energy CT for the assessment of traumatic bone marrow edema of the scaphoid, Eur. Radiol. 31 (7) (2021) 4428–4437.
[25] E.L. Nickoloff, F. Feldman, J.V. Atherton, Bone mineral assessment: new dual-energy CT approach, Radiology 168 (1) (1988) 223–228.
[26] S. Wesarg, M. Kirschner, M. Becker, M. Erdt, K. Kafchitsas, M.F. Khan, Dual-energy CT-based assessment of the trabecular bone in vertebrae, Methods Inf. Med. 51 (5) (2012) 398–405.
[27] Q.Y. Wang, N. Ding, Y.H. Dong, Z.X. Wen, R. Chen, S.Y. Liu, et al., Pharmacological treatment of osteoporosis in elderly people: a systematic review and meta-analysis, Gerontology. 67 (6) (2021) 639–649.
[28] J.P. van den Bergh, P. Szulc, A.M. Cheung, M. Bouxsein, K. Engelke, R. Chapurlat, The clinical application of high-resolution peripheral computed tomography (HR-pQCT) in adults: state of the art and future directions, Osteoporos Int. 32 (8) (2021) 1465–1485.
[29] M.A. Bredella, S.M. Daley, M.K. Kalra, J.K. Brown, K.K. Miller, M. Torriani, Marrow adipose tissue quantification of the lumbar spine by using dual-energy CT and single-voxel (1)H MR spectroscopy: a feasibility study, Radiology 277 (1) (2015) 230–235.
[30] M. Shojaa, S. Von Stengel, D. Schoene, M. Kohl, G. Barone, L. Bragonzoni, et al., Effect of exercise training on bone mineral density in post-menopausal women: a systematic review and meta-analysis of intervention studies, Front Physiol. 11 (2020) 652.
[31] Q. Zaidi, O.A. Danisa, W. Cheng, Measurement techniques and utility of hounsfield unit values for assessment of bone quality prior to spinal instrumentation: a review of current literature. Spine (Phila Pa 1976). 2019;44(4):E239-E44.
[32] T. Helfen, C.M. Sprecher, U. Eberli, B. Gueorguiev, P.E. Muller, R.G. Richards, et al., High-Resolution tomography-based quantification of cortical porosity and cortical thickness at the surgical neck of the humerus during aging, Calcif Tissue Int. 101 (3) (2017) 271–279.
[33] S. Niempoog, S. Sukkarnkosol, K. Boontanapibul, Prevalence of osteoporosis in patients with distal radius fracture from low-energy trauma, Malays Orthop J. 13 (3) (2019) 15–20.
[34] L.D. Gruenewald, C. Booz, S.S. Martin, et al., Diagnostic performance of modern computed tomography in cruciate ligament injury detection: A comprehensive study, Eur. J. Radiol. (2023), https://doi.org/10.1016/j.ejrad.2023.111235. Published online 30 (November).